High Core Electron Confinement Regimes in FTU Plasmas with Low- or Reversed-Magnetic Shear and High Power Density Electron-Cyclotron-Resonance Heating

P. Buratti, E. Barbato, G. Bracco, S. Cirant,* F. Crisanti, G. Granucci,* A. A. Tuccillo, V. Zanza, M. Zerbini,
L. Acitelli, F. Alladio, B. Angelini, M. L. Apicella, G. Apruzzese, L. Bertalot, A. Bertocchi, M. Borra, A. Bruschi,*
G. Buceti, A. Cardinali, C. Centioli, R. Cesario, C. Cianfarani, S. Ciattaglia, V. Cocilovo, R. De Angelis, F. De Marco,
B. Esposito, D. Frigione, L. Gabellieri, G. Gatti, E. Giovannozzi, C. Gourlan, M. Grolli, A. Imparato, H. Kroegler,
M. Leigheb, L. Lovisetto, G. Maddaluno, G. Maffia, M. Marinucci, G. Mazzitelli, P. Micozzi, F. Mirizzi, S. Nowak,*
F. P. Orsitto, D. Pacella, L. Panaccione, M. Panella, V. Pericoli Ridolfini, L. Pieroni, S. Podda, G. B. Righetti,
F. Romanelli, F. Santini, M. Sassi, S. E. Segre,† A. Simonetto,* C. Sozzi,* S. Sternini, O. Tudisco, V. Vitale,
G. Vlad, and F. Zonca

Associazione EURATOM-ENEA sulla Fusione, Centro Ricerche Frascati, CP 65-00044, Frascati, Roma, Italy
(Received 4 June 1998)

Electron temperatures in excess of 8 keV have been obtained by electron-cyclotron-resonance heating on FTU plasmas at peak densities up to 8×10^{19} m^{-3}. The magnetic shear in the plasma core is low or negative, and the electron heat diffusivity remains at, or below, the Ohmic level (0.2 m^2/s), in spite of the very large heating power density (10−20 MW/m^3) which produces extremely high temperature gradients (up to 120 keV/m). The ion heat transport remains at the neoclassical level. [S0031-9007(98)08217-9]

Recent experiments on tokamak configurations with low- or reversed-magnetic shear have obtained transitions to improved confinement regimes. In a toroidal configuration with nested magnetic surfaces, the magnetic shear s is a measure of the radial variation of the safety factor q, i.e., of the field lines winding index. If the magnetic surfaces are labeled by the enclosed volume V, the magnetic shear is defined by $s = (2V/q)(dq/dV)$, so that shear reversal (i.e., negative shear in the plasma core) implies the presence of an off-axis minimum in the q profile. The formation of internal transport barriers (ITB) for particles, ion heat, and momentum transport has been mostly observed in experiments with predominant ion heating [1–7]. The behavior of electron heat transport is a critical issue for the attractiveness of reversed shear configurations in ignited plasma regimes, where α-particle heating raises the electron temperature (T_e) above the ion temperature (T_i). In experiments with predominant ion heating the ITB formation is accompanied by a clear reduction of the electron heat diffusivity only in some cases [7]; furthermore, in these experiments T_i/T_e ranges from 1.5 to 4, so that experiments with direct electron heating are needed to study the electron heat transport in a regime appropriate for a reactor.

Reversed shear configurations have been obtained in experiments with predominant electron heating, either by off-axis lower hybrid current drive [8–11] or by off-axis electron cyclotron resonance heating, which produced hollow temperature profiles in the presence of strong central losses [12]. In the first case, a strong improvement of the electron energy confinement was found for values of the local magnetic shear below 0.05, whereas, in the second case, a local transport barrier was observed to form at the minimum q radius, when the minimum q value fell just below 3. In both cases, a large part of the auxiliary heating was deposited outside the region of improved confinement, in order to control the shape of the q profile.

In this Letter we report the first experiments in which electron-cyclotron-resonance heating (ECRH) at 140 GHz was used during fast current ramps, in order to obtain inverted or flat q profiles by exploiting the skin effect. This experimental scheme has two main advantages: all the auxiliary heating power is absorbed in a small volume well within the region of negative or low-magnetic shear, and the effect of magnetic shear on transport can be studied at a fixed power deposition profile. In addition, the high power density allowed one to explore the heat flux dependence on $n_e \nabla T_e$ (n_e being the electron density) over a range expanded by a factor of 5 compared to other experiments with electron heating.

The experiments were carried out on the FTU tokamak [13] (major radius $R_0 = 0.935$ m, minor radius $a = 0.3$ m, molybdenum toroidal limiter, stainless steel liner). Up to 360 kW of ECRH power were injected at the fundamental frequency [14]. Magnetic shear reversal was obtained owing to the fast current ramp rate (5–7 MA/s) and to the skin effect enhanced by the high electron temperatures (in excess of 8 keV).

The evolution of the electron temperature profile is measured on FTU by means of second harmonic electron cyclotron emission (ECE) and Thomson scattering (TS) diagnostics [15,16]. ECE is collected along a major radius on the equatorial plane and analyzed by an absolutely calibrated Michelson interferometer with a 5 ms time resolution. Stray radiation from the gyrotron is efficiently

rejected by a notch filter tuned to 140 GHz. Fast ECE measurements (25 μs time resolution) are also given by a 12-channel grating polychromator.

Temporal evolution of a typical deuterium discharge is shown in Fig. 1. The toroidal magnetic field at $R = R_0$ was set at $B_0 = 5.2$ T in order to have the resonance ($B = 5$ T) close to the magnetic axis ($R_{ax} = 0.97$ m). Temperature and density at the beginning of the ECRH pulse ($t = 55$ ms) were $T_e(R_{ax}) = 1$ keV and $n_e(R_{ax}) = 3 \times 10^{19}$ m^{-3}. The excellent agreement between ECE and TS data [see Fig. 1(c)] and the absence of suprathermal features in ECE spectra confirmed that the ECRH power was fully absorbed by thermal electrons.

ECRH experiments have been performed at different values of the toroidal field in order to find the optimum heating conditions and to check the effect of off-axis heating. At $B_0 = 5.4$ T the resonance was shifted by 3.7 cm, and the profile shape changed significantly during the transient [Fig. 2(b)], but the increasing Shafranov shift drove the magnetic axis towards the resonance position, leading to nearly central heating at the end of the temperature rise. With a further displacement of the resonance ($B_0 = 5.6$ T), hollow profiles were produced in the transient phase, while the steady state profile was flat in the central region and had the maximum gradient close to the resonance position [Fig. 2(c)]. In contrast, no significant changes were observed in the density profiles. These results indicate that the electron heat transport has an essentially diffusive response to the power deposition profile, i.e., that, at least in the central region of reversed shear configurations, there is no profile resiliency. The

existence of a strong heat pinch can be excluded as well, while attempts to reproduce the off-axis heating results by a purely diffusive transport model revealed that a small heat pinch could indeed be present. The evidence of local rather than global transport is consistent with the expected decrease of the turbulence radial correlation length with low- or negative magnetic shear [17].

The power balance in the central region of the discharges shown in Figs. 2(a) and 2(b) is dominated by ECRH; this allows one to perform an accurate analysis of the electron heat transport in plasmas with reversed-magnetic shear and large values of the heat flux.

The electron thermal diffusivity χ_e is evaluated according to

$$\langle \mathbf{q}_e \nabla \rho \rangle = -\chi_e n_e \langle |\nabla \rho|^2 \rangle \frac{\partial T_e}{\partial \rho} .$$

FIG. 1. Time evolution of (a) plasma current, (b) line average electron density, and (c) electron temperature for FTU pulse No. 12799. The solid line in (c) represents the fast ECE measurement at $R = 0.976$ m, the circles give Thomson scattering results at $R = 0.965$, and the triangles represent the peak temperature as measured by the Michelson interferometer.
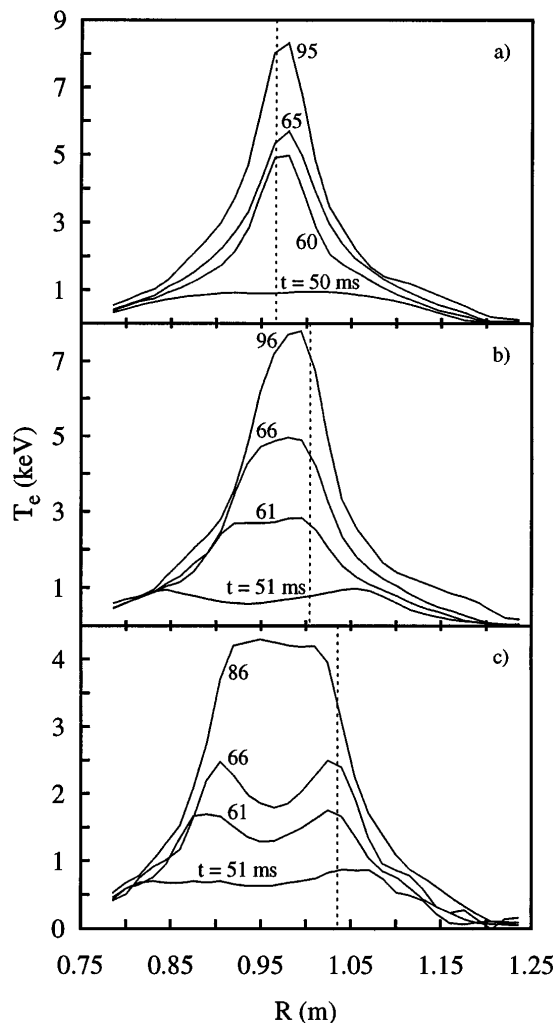
FIG. 2. Evolution of the electron temperature profile for different values of the toroidal field: (a) $B_0 = 5.2$ T (pulse No. 12799); (b) $B_0 = 5.4$ T (pulse No. 12658); (c) $B_0 = 5.6$ T (pulse No. 12952). ECRH is applied at $t = 55$ ms; the resonance location is marked by a dashed vertical line.

The left-hand side is the normal electron heat flux averaged on the magnetic surface, and the effective flux surface radius ρ is defined from the toroidal flux Φ_T according to $\rho = \sqrt{\Phi_T/\pi B_0}$. The magnetic surfaces are given by an equilibrium reconstruction code. The heat flux is evaluated from the electron power balance equation,

$$\langle \mathbf{q}_e \nabla \rho \rangle = (P_{EC} + P_{Ohm} - P_{ei} - P_{RAD}$$
$$- \partial W/\partial t)/V',$$

which accounts for power sources and sinks within the magnetic surface: P_{EC} is the ECRH power; P_{Ohm} is the Ohmic dissipation; P_{ei} and P_{RAD} give electron-ion equipartition and radiation losses, respectively; W is the electron thermal energy; and $V' = \partial V/\partial \rho$.

Figure 3 shows the q-profile evolution for pulse No. 12658 [see Fig. 2(b)]. The profiles are obtained from the solution of the magnetic field diffusion equation, starting with a relaxed current density profile at $t = 51$ ms, i.e., neglecting the skin effect in the low temperature phase which precedes the ECRH injection. The accuracy of the q profiles can be evaluated by exploiting the precursor of an $m = 2$, $n = 1$ double tearing relaxation observed at $t = 106.5$ ms [18]: the temperature modulation profile points to the existence of a pair of $q = 2$ surfaces at about 0.15 and 0.45 normalized radius, while the calculated q profile at $t = 106$ ms has a single resonance at 0.35; this implies that the calculation underestimates the extent of the negative shear region.

The source and loss terms of the power balance are shown in Fig. 4(a) for the time slice at $t = 96$ ms. The
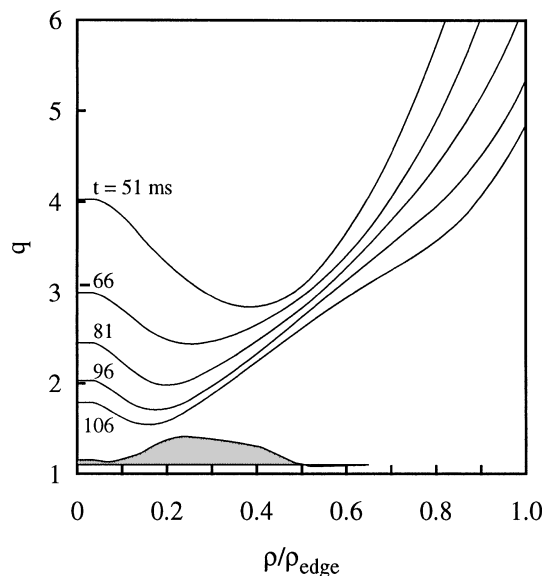
Ohmic power is calculated for a range of Z_{eff} values, since the choice of a uniform $Z_{eff} = 6.7$ with Spitzer resistivity reproduces the loop voltage in the Ohmic phase, while $Z_{eff}(0) = 9$ is given by the analysis of soft x-ray spectra from highly ionized charged states of metallic impurities. These high Z_{eff} values, which are not typical of FTU operation, can be attributed to the extremely low values of the $\overline{n}_e/I_p$ ratio ($\overline{n}_e$ and I_p being line average density and plasma current, respectively) reached during fast current ramps [19]; discharges with slower ramp rate and lower Z_{eff} yielded qualitatively similar ECRH effects, but were affected by earlier sawtooth relaxations. The total calculated Ohmic power increases from 0.8 to 1.4 MW (the integrated Poynting flux being 3.5 MW) if Z_{eff} is increased from 6.7 to 9, and neoclassical resistivity is introduced. The corresponding variation of the P_{Ohm} profile is represented by the shaded area in Fig. 4(a). The uncertainty is large in the outer midradius, so that it affects the evaluation of the global energy confinement time, while the core heat diffusivity remains a robust figure.

The P_{EC} profile is calculated by a ray tracing code interfaced with the equilibrium reconstruction. The effect of wall reflections has been neglected since 99% of the launched power is absorbed at the first pass. The power balance is dominated by the ECRH source term

FIG. 3. Time evolution of the q profile calculated for pulse No. 12658 assuming $Z_{eff} = 6.7$ and Spitzer resistivity. ρ_{edge} is the radial coordinate of the last closed magnetic surface. The shaded area shows the temperature modulation (in units of keV, with a baseline offset at 1.1) during the growth of an $m = 2$ double tearing instability.
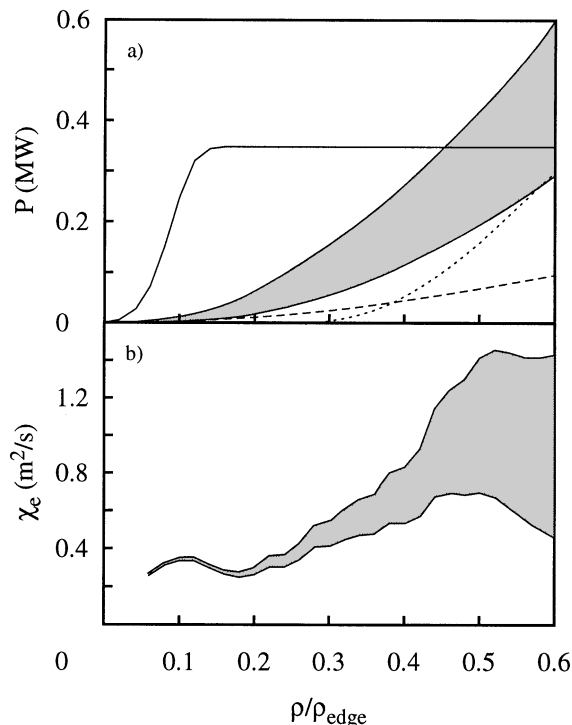
FIG. 4. (a) Radial profiles of source and sink terms of the electron power balance for pulse No. 12658 at $t = 96$ ms. Solid line: ECRH source term; shaded area: Ohmic power; dotted line: radiated power; dashed line: electron-ion equipartition power. (b) Radial profile of the electron heat diffusivity. The shaded area represents the uncertainties arising from the Ohmic power calculation.
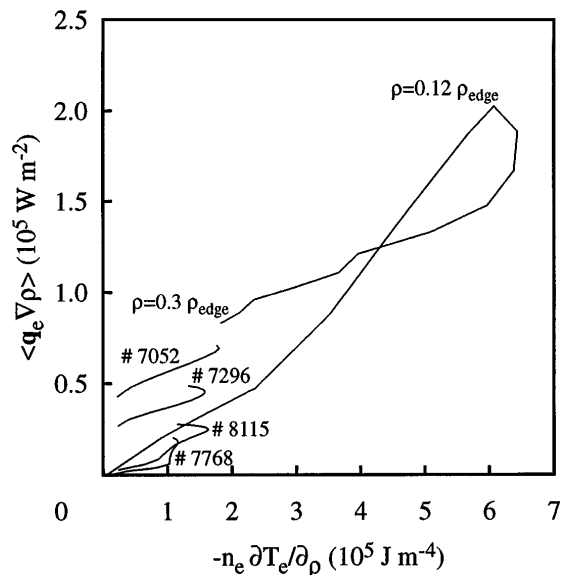
FIG. 5. Flux surface averaged normal electron heat flux vs $-n_e \partial T_e/\partial \rho$ for pulse No. 12658 at $t = 96$ ms, for two equivalent Ohmic pulses (No. 7052, $t = 880$ ms; No. 7296, $t = 980$ ms), and for two Ohmic pulses at $I_p = 0.35$ MA with very low thermal diffusivity (No. 7768, $t = 840$ ms; No. 8115, $t = 1$ s). Apart from a geometric factor close to 1, χ_e is the ratio between the plotted quantities. Data are shown for $\rho \leq 0.3\rho_{\text{edge}}$.

for $\rho/\rho_{\text{edge}} < 0.4$, with ρ_{edge} being the effective radius of the last closed magnetic surface. The main uncertainty on the P_{EC} profile arises from the determination of the magnetic axis position, which is accurate to within 1 cm. The P_{RAD} profile is given by the inversion of line integrated radiation losses measured by a 16-channel bolometer array. The rate of electron-ion energy transfer (P_{ei}) is calculated by solving the neoclassical ion energy balance equation with Chang-Hinton ion thermal diffusivity [20]. The calculated ion temperature remains below 1.1 keV.

The electron thermal diffusivity profile is shown in Fig. 4(b). The uncertainties arising from the Ohmic power evaluation, represented by the shaded area in the figure, are reasonably low for $\rho/\rho_{\text{edge}} < 0.4$. The profile is cut for $\rho/\rho_{\text{edge}} < 0.06$, where the uncertainties on P_{EC} are relevant. The evaluation of temperature gradients introduces errors due to the calibration accuracy and to the $T_e(\rho)$ determination; in particular, the latter gives a systematic gradient underestimate (by about 20%) that is ignored in the analysis. Within one third of the plasma radius, the diffusivity stays below 0.4 m^2/s and has a minimum at $\chi_e \approx 0.2$ m^2/s; such values are close to the lowest ones found in Ohmic discharges, but have now been obtained in the presence of much larger fluxes and gradients. In order to illustrate this finding, the electron heat flux versus $-n_e \partial T_e/\partial \rho$ plots are overlaid in Fig. 5 for pulse No. 12658 at $t = 96$ ms (at this time $I_p = 0.5$ MA and $\overline{n}_e = 4 \times 10^{19}$ m^{-3}), and for two typical Ohmic, steady state discharges with similar current and density. Two steady state discharges which show the lowest χ_e values in the FTU Ohmic database are also shown for comparison.

In conclusion, the electron transport properties of plasmas with low or negative shear in the plasma core have been studied on the FTU tokamak employing an ECRH auxiliary heating system with a very high power density. A radial scan of the resonance position has shown that the heat transport is mainly diffusive in the plasma core. With central heating, the electron thermal diffusivity remains at the Ohmic level, although the heating power density is increased by an order of magnitude. These results have been obtained in plasmas with $T_e \gg T_i$; this regime is not reactor relevant, but it allows one to single out electron heat transport driven by electron free energy.

*Associazione Euratom-ENEA-CNR, Istituto di Fisica del Plasma, Milano, Italy.

†INFM and Dipartimento di Fisica, II Università di Roma "Tor Vergata," Rome, Italy.

[1] F. M. Levinton *et al.,* Phys. Rev. Lett. **75**, 4417 (1995).
[2] E. J. Strait *et al.,* Phys. Rev. Lett. **75**, 4421 (1995).
[3] T. Fujita *et al.,* Phys. Rev. Lett. **78**, 2377 (1997).
[4] T. T. C. Jones and the JET Team, Phys. Plasmas **4**, 1725 (1997).
[5] Y. Koide and the JT-60 Team, Phys. Plasmas **4**, 1623 (1997).
[6] C. M. Greenfield *et al.,* Phys. Plasmas **4**, 1596 (1997).
[7] K. H. Burrell, Phys. Plasmas **4**, 1499 (1997).
[8] X. Litaudon *et al.,* Plasma Phys. Controlled Fusion **38**, 1603 (1996).
[9] A. A. Tuccillo *et al.,* in *Radio Frequency Power in Plasmas,* edited by P. M. Ryan and T. Intrator, AIP Conf. Proc. No. 403 (AIP, New York, 1997), p. 121.
[10] A. Ekedahl *et al.,* in *Radio Frequency Power in Plasmas* (Ref. [9]), p. 169.
[11] I. Voisekhovitch *et al.,* Nucl. Fusion **37**, 1715 (1997).
[12] M. R. de Baar *et al.,* Phys. Rev. Lett. **78**, 4573 (1997).
[13] R. Andreani *et al.,* in *Proceedings of the 16th Symposium on Fusion Technology, London, 1990* (North-Holland, Amsterdam, 1990), Vol. 1, p. 218.
[14] S. Cirant *et al.,* in *Proceedings of the 10th Joint Workshop on ECE and ECRH,* edited by T. Donnè and T. Verhoeven (World Scientific, Singapore, 1997), p. 369.
[15] P. Buratti and M. Zerbini, Rev. Sci. Instrum. **66**, 4208 (1995).
[16] F. Orsitto *et al.,* Rev. Sci. Instrum. **66**, 2 (1995).
[17] F. Romanelli and F. Zonca, Phys. Fluids B **5**, 4081 (1993).
[18] P. Buratti *et al.,* Plasma Phys. Controlled Fusion **39**, B383 (1997).
[19] M. L. Apicella *et al.,* Nucl. Fusion **37**, 381 (1997).
[20] C. S. Chang and F. L. Hinton, Phys. Fluids **29**, 3316 (1986).